Electronic Supplementary Information for:

Modulating the n- and p-type Photoelectrochemical Behavior of Zinc Copper Indium Sulfide Quantum Dots by an Electrochemical Treatment

Néstor Guijarro,* Teresa Lana-Villarreal and Roberto Gómez*

Institut Universitari d'Electroquímica i Departament de Química Física, Universitat d'Alacant, Apartat 99, E-03080 Alacant, Spain.

*Corresponding authors. E-mails: nestor.guijarro@ua.es, roberto.gomez@ua.es

FAX: (+) 34 965903537; Phone: +34 965903748 (Roberto Gómez)

1.- Synthesis and characterization of Zinc Copper Indium Sulfide colloidal QDs

Zinc Copper Indium Sulfide ($Zn_xCu_yIn_zS_{x+(y/2)+(3z/2)}$) (ZCIS) QD colloidal dispersions were prepared by following the procedure of Nakamura et. al[1] with minor changes. In flask A, 0.099 g of CuCl (Sigma-Aldrich) and 0.22 g of $InCl_3$ (Sigma-Aldrich, 98%) were dissolved in 6 ml of oleylamine (Aldrich, Technical grade 70%) by stirring and mild heating. In flask B, 0.18 g of zinc diethyldithiocarbamate were dissolved in 6 ml of Trioctylphosphine (Sigma-Aldrich) by stirring, adding subsequently 24 ml of Octadecene (Sigma-Aldrich, technical grade 90%). Once the precursors were dissolved, the content of flask A was injected into flask B. The mixture was gently heated, while the temperature inside the flask was monitored. The color of the dispersion changes from yellow to dark brown when temperature rises from 115 to 155 ºC, mainly because of the loss of quantum confinement when the particle size increases. All the samples used in this work were prepared by cooling down to ambient temperature the reaction flask when it reached 140 ºC (absorption and emission spectra of the product have proven to be rather reproducible among different batches). All processes were carried out under N_2 atmosphere and reagents were employed without further purification.

The as-synthesized QDs were washed by precipitating them with a mixture 1:4 CH_2Cl_2:EtOH, followed by centrifugation to remove the excess of reagents, and finally by redispersing them in CH_2Cl_2. Usually, 4 ml of colloidal dispersion were washed with 8 ml of CH_2Cl_2:EtOH, and redissolved in 1 ml CH_2Cl_2. It is important to remark that repetition of the washing process yield insoluble particles, likely due to an irreversible loss of the capping agent.

The QD composition was determined by means of Inductively Coupled Plasma Mass Spectrometry (ICP-MS) with a VGPQ-Excell spectrometer from Thermo Elemental. For this purpose, the colloidal dispersion was washed as mentioned above, but dissolving the pellet obtained at the bottom of the centrifuge tube with a small volume of a mixture H_2O:H_2O_2:HNO_3:H_2SO_4 (2:2:2:1) and adding 2 % HNO_3 solution up to the desired volume. All the samples were filtered (0.45 µm) prior to analysis. Table S1 summarizes the results.

Table S1. Summary of the results obtained by ICP-MS

	Concentration[a] / mol mL^{-1}	Elemental ratio
Cu	$1.865 \cdot 10^{-6}$	1
In	$8.035 \cdot 10^{-6}$	4.3
Zn	$2.485 \cdot 10^{-6}$	1.3

[a] Concentration of the dispersion employed for the photocurrent transient experiments

According to the obtained values, the composition for the ZCIS QDs would be $Zn_{1.3}CuIn_{4.3}S_{8.25}$. The high indium content is not unexpected given the wide range of compositions reported in the literature.[1-4] Furthermore, the ratio Cu/Zn agrees with the value previously reported by Nakamura et al.[1] despite the changes in the synthesis procedure.

Assuming spherical QDs of 3.5 nm in diameter (as measured from TEM images) and a density of 4.67 $g \cdot cm^{-3}$ for the nanocrystals (as reported for bulk $CuInS_2$),[2] the mass of each QD would be 10^{-19} g. Taking into account the experimental concentration found for each component the concentration of the colloidal QD solution can be estimated as $1.6 \cdot 10^{16}$ mL^{-1}.

The ZCIS QDs were structurally characterized by Raman spectroscopy. The band obtained between 300-350 cm^{-1} has already been reported by other authors for copper-deficient $CuInS_2$ nanocrystals.[5,6] Importantly, neither signals at 475 cm^{-1} due to Cu_xS,[4] nor at 244 cm^{-1}, which would be attributed to β-In_2S_3[7] are observed. In the same way, no signals are detected at 179 or 262 cm^{-1}, which would be ascribed to polycrystalline In_2S_3.[8] However, the presence of ZnS cannot be completely ruled out as its Raman spectrum frequently shows only one predominant peak at around 320 cm^{-1}.[9]

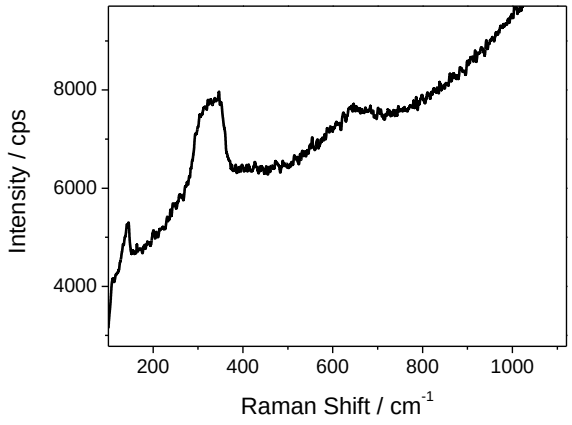

Figure S1. Raman spectra of ZCIS QDs deposited on glass.

In order to obtain a more complete picture of the ZCIS QD composition, the XPS was measured, as shown in figure S2. The survey spectrum indicates the presence of Cu, In, S, C and O. The presence of C and O is likely due to the capping agents and contamination resulting from exposure to the atmosphere. The Zn2p, Cu2p, In3d and S2p core levels were examined to reveal the valence state. The Zn 2p spectrum is composed of two states (2p3/2 and 2p1/2), at 1021 and 1041 eV, being consistent with a valence of +2 and in good agreement with values reported for Zn^{2+} in environments such as zinc sulfide[10] or $ZnIn_2S_4$.[11] For the Cu2p core level spectrum, two separate peaks located at binding energies of 931.5 eV and 951 eV are attributed to Cu2p3/2 and 2p1/2, respectively, in agreement with literature values for Cu^{+}.[12,13] The absence of a satellite peak at 942 eV, indicates the absence of Cu^{2+}.[14] Similarly, In3d shows two peaks at 444.1 and 451.7 eV, being consistent with a valence of +3.[12,13] The S2p peak can be assigned to S coordinated with Cu, In and Zn.

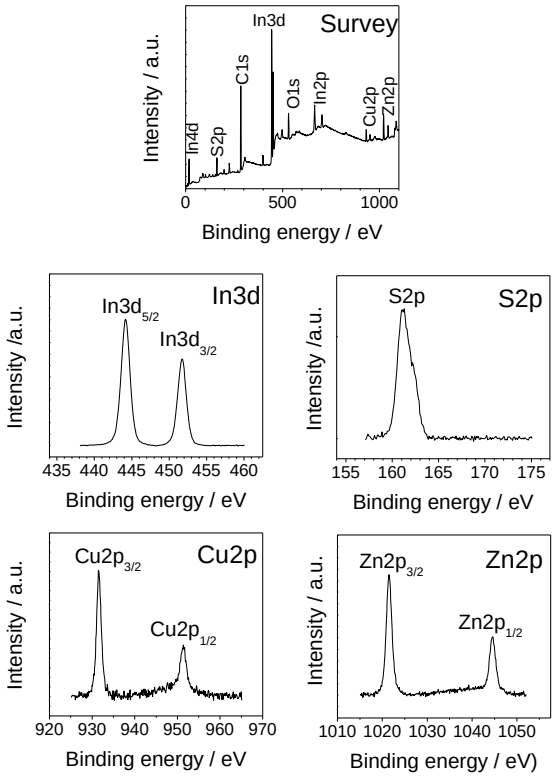

Figure S2. XPS spectra for the as-synthesized ZCIS QDs. The survey spectrum and the spectra for In3d, S2p, Cu2p and Zn2p are shown.

2.- Working electrode preparation (FTO/ZCIS or Au/ZCIS)

ZCIS colloidal QDs were deposited on conductive substrates, either FTO or gold, (the latter only for QCM measurements) by drop casting and subsequent immersion in ethanol for 15 s to improve the assembly. In particular, photocurrent experiments were performed by drop casting 40 $\mu L \cdot cm^{-2}$ of the as-prepared QD dispersion, whereas for cyclic voltammetry, emission spectroelectrochemistry and QCM measurements 16 or 20 $\mu L \cdot cm^{-2}$ of a diluted sample was employed (see below).

3.-Electrochemical measurements

3.1- Electrochemical and photoelectrochemical measurements

Photocurrent transients and cyclic voltammetry were performed at room temperature in a three electrode cell equipped with a quartz window, using an Autolab PGSTAT30 potentiostat. An Ag/AgCl/KCl (sat.) electrode and a Pt wire were used as reference and counter electrodes, respectively. Both, N_2-purged aqueous polysulfide (1 M Na_2S + 1 M NaOH + 0.1 M S) and 5 mM Na_2S+ 1 M NaOH were used as electrolytes. Cyclic voltammetry was performed at 10 $mV \cdot s^{-1}$ in all cases. For the photoelectrochemical measurements, modified FTO electrodes were illuminated from the electrolyte side using a 300 W Xe arc lamp (Oriel) with a UV filter (approx. irradiance 70.0 $mW \cdot cm^{-2}$).

3.2.- Emission spectroelectrochemical experiments

A typical cuvette used for emission spectroscopy was adapted to allow for the introduction of the different elements of a conventional three-electrode cell. Subsequently, it was accommodated into the sample holder of the spectrofluorometer (Fluoromax-4) to measure "in situ" the working electrode emission spectra. The excitation wavelength was 450 nm, and the emission kinetic was monitored at 700 nm while the potential was controlled simultaneously by a µAutolab III (EcoChemie 3 B. V.). The electrolyte was 5 mM Na_2S + 1 M NaOH.

3.3.- Electrochemical Quartz Crystal Microbalance measurements

A QCM200 microbalance controller from Stanford Research Systems (SRS) was coupled to the potentiostat employed for the electrochemical measurement through the Crystal Face Bias connection at the QCM25. Commercial quartz crystal sensors (SRS) consisting of 5 MHz quartz with circular Cr/Au electrodes patterned on both sides were employed. Prior to the

electrochemical measurements, the probe was air-equilibrated. A clear diminution in the frequency was detected during the QD casting, directly ascribed to the mass increase associated with QD deposition. Subsequently, the crystal holder was introduced in the electrochemical cell using 1 M NaOH + 5 mM Na_2S aqueous solution as electrolyte. Once the probe was equilibrated and stabilized, the electrochemical measurements were performed with an Autolab PGSTAT30, simultaneously monitoring the frequency. Due to the small amount of QDs deposited, we can consider a rigid behavior for the electrode and employ the Sauerbrey equation to estimate the mass change. (The sensitivity factor for the employed crystals was equal to 56.6 Hz μg^{-1} cm^2.

4.- QD modification in dilute sulfide solutions

A polysulfide electrolyte completely quenches the photoluminescence of the ZCIS QDs and strongly adsorbs on a gold electrode, hampering studies addressed to uncover the modification mechanism. A more suitable electrolyte, such as 1 M NaOH + 5 mM Na_2S, was employed to perform cyclic voltammetry, emission spectroelectrochemistry and electrochemical QCM analysis. It is worth mentioning that after the first scan the current drops dramatically, suggesting that most of the doping has been already attained (figure S3A). To ensure that the modification is occurring as in polysulfide, a FTO/ZCIS electrode was prepared and submitted to 0 V for 20 s (electrochemical treatment) in 1 M NaOH + 5 mM Na_2S. Afterward, a photocurrent transient was measured in polysulfide (figure S3B). As expected a cathodic photocurrent was measured. To compare this result with the electrochemical treatment in polysulfide, this treatment was subsequently performed in such a solution. The cathodic photocurrent further increases. This effect is ascribed to a better Cu(II) withdrawal by the surrounding medium.[15,16]

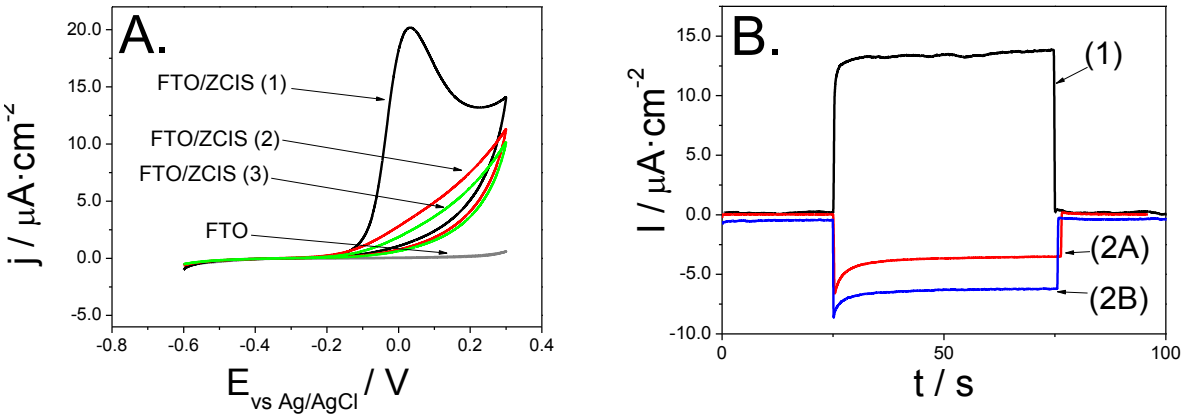

Figure S3. Successive cyclic voltammograms (1st to 3rd) for a ZCIS-modified FTO electrode together with a steady-state voltammogram for a bare FTO electrode recorded at 10 $mV \cdot s^{-1}$ in 1 M NaOH + 5mM Na_2S solution (A). Photocurrent transients for an FTO/ZCIS electrode measured: (1) as-prepared, (2A) after the electrochemical treatment in 1 M NaOH + 5mM Na_2S, and (2B) after an additional treatment in polysulfide. The measurements were carried out in three-electrode cells using polysulfide (1 M Na_2S + 1M NaOH + 0.1 M S) as electrolyte at -0.7 V (B).

It is remarkable that a much lower degree of modification is attained when the electrochemical treatment is performed in 1 M NaOH (figure S4). However, in such a case the lack of sulfide ions increases the instability of the QDs (i.e. corrosion and detachment of the QD film) giving rise to irreproducible results.

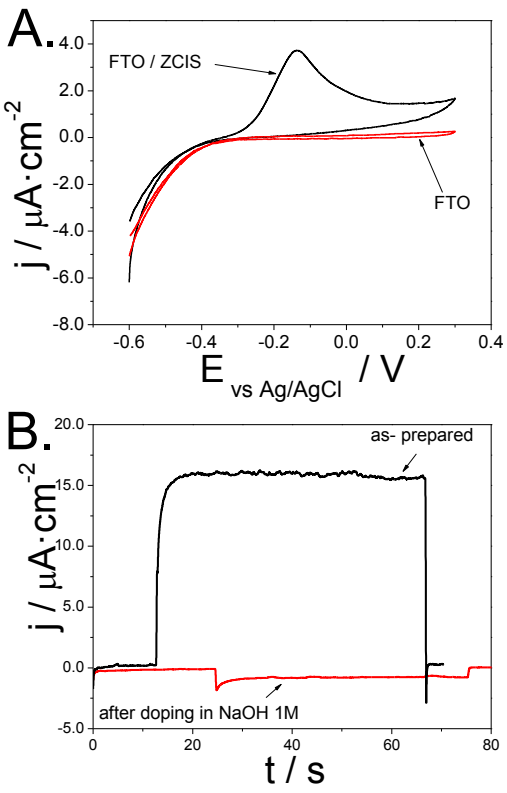

Figure S4. Cyclic voltammetry (A) and photocurrent transients (B) of FTO/ZCIS electrodes. Cyclic voltammetry was performed at 10 $mV \cdot s^{-1}$ in 1 M NaOH, whereas photocurrent transients were performed as described in Figure S3.

5.- Effect of the deposited QD loading on cyclic voltammetry

The as-prepared ZCIS QD colloidal dispersion was diluted several times (table S2). FTO/ZCIS electrodes prepared by drop casting 16 $\mu L \cdot cm^{-2}$ (8 µL per 0.5 cm^2) were analyzed by cyclic voltammetry. The charge (Q) involved in the oxidation process is determined (Table S2) and plotted as a function of the QD loading in Fig. S5. The charge progressively increases with the QD loading until it saturates evidencing that only the QDs placed near the substrate undergo modification, while the outermost layers remain electrochemically inactive. We can calculate the number of equivalent QD monolayers (N_L) in each electrode using the data of Table S2, i.e. the amount of QDs deposited, and considering that the QD are arranged in a compact hexagonal structure. In such a case, assuming that the QD are spherical (3.5 nm in

diameter, according to the TEM), the area occupied by each QD is 10^{-13} cm^2. As the size of the electrode active area was 0.5 cm^2, it means that $5 \cdot 10^{12}$ QDs constitute a monolayer. The number of layers for each sample is also shown in Table S2.

Table S2. ZCIS concentration of the samples used for the preparation of FTO/ZCIS electrodes, and the calculated number of deposited QDs and layers. Area: 0.5 cm^2

Sample	Concentration / mL^{-1}	QDs deposited	Charge / µC	QD layers
Fresh	$1.6 \cdot 10^{16}$	$1.3 \cdot 10^{14}$	423.0	27.0
A	$5.3 \cdot 10^{15}$	$4.3 \cdot 10^{13}$	412.4	9.0
B	$1.8 \cdot 10^{15}$	$1.4 \cdot 10^{13}$	304.7	3.0
C	$5.8 \cdot 10^{14}$	$4.6 \cdot 10^{12}$	226.2	1.0
D	$2.9 \cdot 10^{14}$	$2.4 \cdot 10^{12}$	148.5	0.5
E	$1.48 \cdot 10^{14}$	$1.2 \cdot 10^{12}$	103.2	0.25

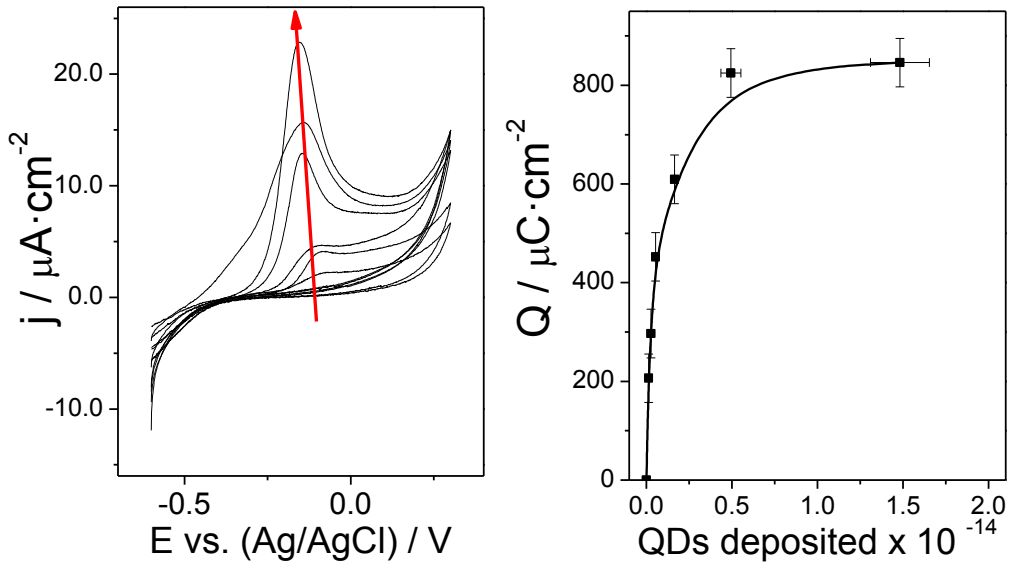

Figure S5. Cyclic voltammetry for FTO/ZCIS electrodes prepared with different concentration of the colloidal dispersion (left) and the integrated charge density corresponding to the oxidation process (right). Cyclic voltammetry was carried out at 10 $mV \cdot s^{-1}$ in 5mM Na_2S + 1 M NaOH.

If we assume that the oxidation process is limited to the first layer of QDs directly in contact with the FTO, the charge should be directly proportional to the number of QDs in contact with the substrate. When a very small amount of QDs is deposited, most of them should be in direct contact with the FTO and, therefore, electroactive. If we plot the tangent of the Q vs. N_L curve at the origin, we realize that it attains the saturation charge at an N_L value approximately equal to one (see fig. S6). This result clearly points to the fact that exclusively the first QD monolayer is electroactive.

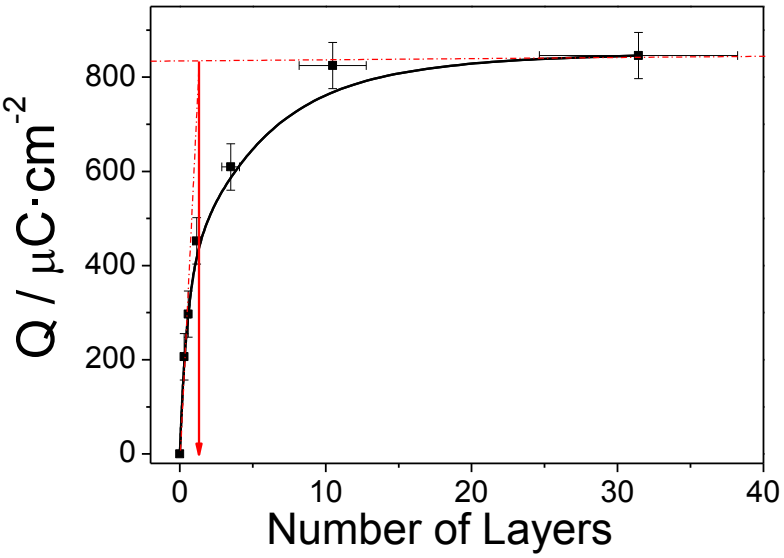

Figure S6. Charge density corresponding to the oxidation process (Figure S5) as a function of the number of deposited equivalent monolayers.

In order to make this conclusion more quantitative, we consider that the charge associated with the electrochemical treatment (Q) should be directly proportional to the QD coverage degree (θ) defined as the number of surface sites occupied by QDs (regardless the number of QDs adsorbed per site) divided by the total number of surface sites. We are assuming that the QD assembly is not layer-by-layer. Obviously, the charge would be at a maximum (Q_{max}) when θ tends to 1:

$$Q = Q_{max}\theta \qquad \text{(S1)}$$

In addition:

$$Q = Q_{max}\left(1-\theta_0\right) \tag{S2}$$

being θ_0 the fraction of sites that are uncovered. For a random growth, the fraction of sites with *i* deposited QDs (θ_i) should be proportional to θ_{i-1}:

$$\begin{aligned}\theta_1 &= A\theta_0 \\ \theta_i &= B\theta_{i-1}\end{aligned} \tag{S3}$$

Both proportionality constants (A and B) have values comprised between 0 and 1. We have distinguished between the first monolayer and the rest, as the interaction QD-FTO could be very different from the interaction QD-QD. The number of equivalent monolayers can be calculated as:

$$N_L = \sum_{i=1}^{N} i\theta_i = A\theta_0\left(1+2B+3B^2\ldots\right) = \frac{A}{\left(1-B\right)^2}\theta_0 \tag{S4}$$

and

$$\theta_0 = 1-\sum_{i=1}^{N}\theta_i = 1-A\theta_0\left(1+B+B^2\ldots\right) = 1-\frac{A}{1-B}\theta_0 \tag{S5}$$

By combining equations (S4) and (S5) and defining C as the ratio A/B, one may obtain:

$$N_L = \frac{\left(1-\theta_0\right)\left[\left(1-\theta_0\right)+C-C\left(1-\theta_0\right)\right]}{C-C\left(1-\theta_0\right)} = \frac{Q\left[Q+C\cdot Q_{max}-CQ\right]}{C\cdot Q_{max}\left(Q_{max}-Q\right)} \tag{S6}$$

If C is equal to one, the equation can be simplified to:

$$N_L = \frac{Q}{Q_{max}-Q} \quad \rightarrow \quad \frac{1}{N_L} = \frac{Q_{max}}{Q} - 1 \tag{S7}$$

Figure S7 shows the experimental Q vs. N_L plot, together with the curves fitted according to (S7).

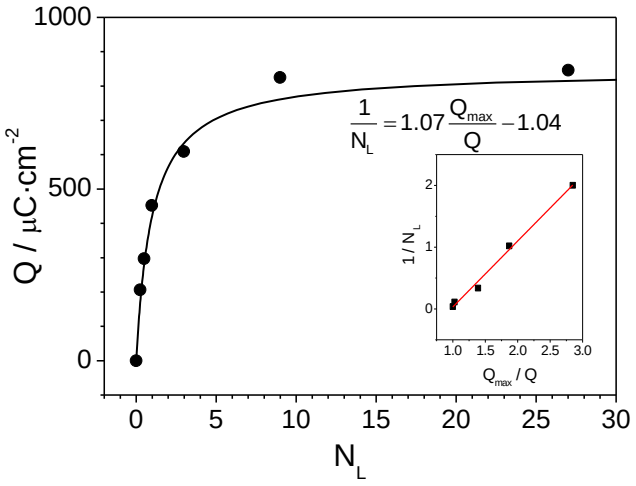

Figure S7. Charge corresponding to the cyclic voltammograms in Figure S5 as a function of the equivalent number of deposited monolayers. The solid and the inset show a fit according to eq. S7.

The good fit of the experimental results to eq. S7 and the relatively low charge density values found in all cases strongly indicate that only the first monolayer is electroactive, i.e., sensitive to the electrochemical treatment.

It is noteworthy that in all the experiments the amount of QDs employed was enough to have the maximum response, i.e., a complete first monolayer. In fact, solution A (Table S2) was employed for the preparation of the electrodes used in cyclic voltammetry, emission spectroelectrochemistry and QCM measurements.

6. - Effect of QD modification on the UV-Vis absorption spectrum

Figure S8 shows that the electrochemical treatment does not lead to discernible changes in either the appearance or the absorption spectra of the electrodes.

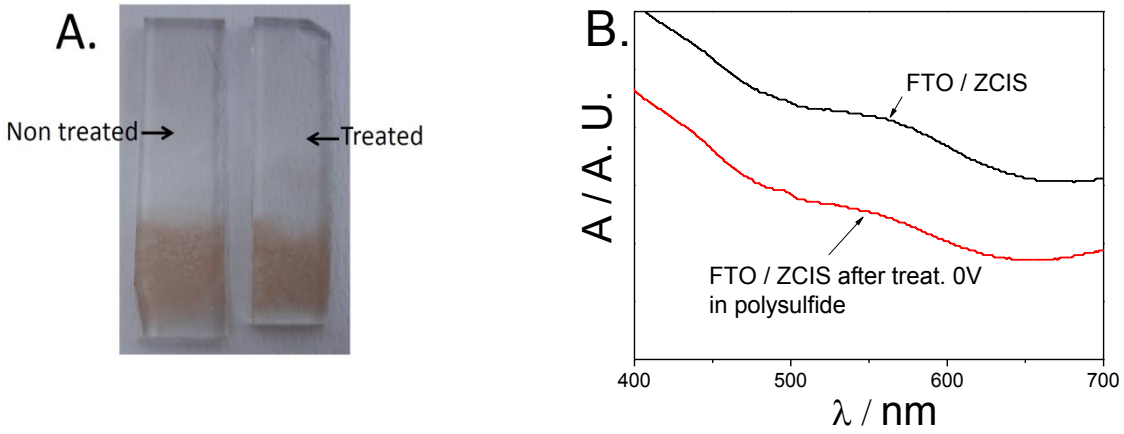

Figure S8. Photograph (A) and UV-Vis absorption spectra (B) of a QD electrode before and after the electrochemical treatment.

7.- Details of the Quartz Crystal Microbalance (QCM) measurements

For the QCM measurements 8 µL of solution A were deposited on a QCM gold substrate covering around 0.5 cm^2. After drop casting the QD solution, an increase in mass of 9 $\mu g \cdot cm^{-2}$ was measured in air. With this value and the mass of each QD (see section 1), we can estimate that the number of QD compact layers is approximately 10. A similar value is also calculated from the volume added and the concentration of the QD dispersion. More importantly, according to the behavior reported in figure S7, the gold surface is likely completely covered. Subsequently, the crystal holder was introduced in an electrochemical cell containing 1 M NaOH + 5 mM Na_2S aqueous solution as electrolyte. Once the probe was equilibrated and stabilized, electrochemical measurements were performed with simultaneous monitoring of the frequency. Cyclic voltammetry of the gold substrate modified with the ZCIS QDs is shown in figure S9. As observed, the first cycle gives rise to a current larger than the second one although, in contrast to experiments carried out using a FTO substrate, the latter is not negligible. Nevertheless, we consider that modification occurs during the first cycle, as confirmed in FTO supported electrodes, while the second cycle current is ascribed to background currents linked to the sulfide/gold system. Therefore, as shown in figure 3 (main

text), two consecutive potential step experiments were performed, the charge of the second transient (706 $\mu C \cdot cm^{-2}$) was subtracted to that of the first one (1422 $\mu C \cdot cm^{-2}$) in order to reckon only the charge involved in modification. In the experiments performed using FTO substrates (Table S2) the charge involved in the modification process for a monolayer is 846 $\mu C \cdot cm^{-2}$, rather similar to the experimental data obtained on gold (716 $\mu C \cdot cm^{-2}$). Such deviations could be explained by the different assemblies induced by the different nature of the substrates and by the fact that modification could not be completed in the first step.

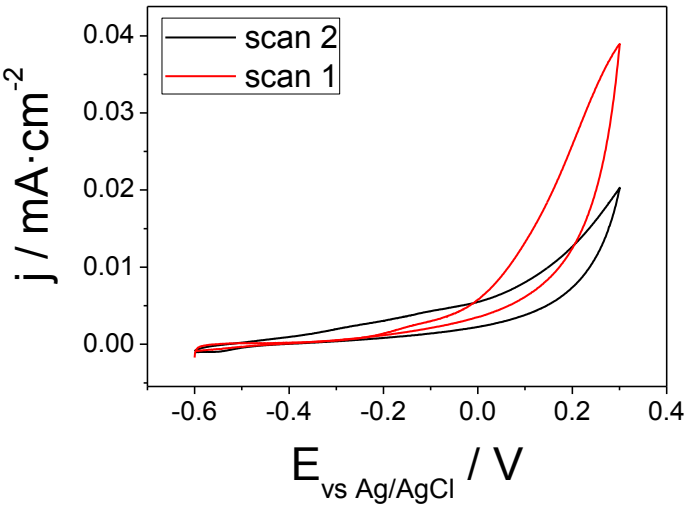

Figure S9. Cyclic voltammetry for QDs supported on the gold electrode of the QCM. Measurements were carried out in 1 M NaOH + 5 mM Na_2S, at 10 $mV \cdot s^{-1}$.

If we ascribed this charge (716 $\mu C \cdot cm^{-2}$) to the oxidation process of Cu (I) to Cu (II), assuming that the latter is subsequently scavenged by complexation with sulfide ions,[16] we can estimate the mass change (Δm) as follows. The charge recorded involves the oxidation of $7.4 \cdot 10^{-9}$ mol of Cu per cm^2, which would correspond to a change in mass of 0.47 $\mu g \cdot cm^{-2}$. This value, although larger, is of the same order of magnitude of the value experimentally obtained (0.17 $\mu g \cdot cm^{-2}$). It is important to remark that these measurements were carried out in a dilute solution of sulfide (1 M NaOH + 5 mM Na_2S), which could hamper the withdrawal of the Cu (II) toward the solution. In addition, the efficient Cu dissolution could be hindered due

to the fact that the electrode is constituted by a multilayer of QDs, only the first monolayer being electroactive.

Finally, we can estimate the percentage of Cu atoms that are oxidized during the treatment. The surface density of Cu atoms can be obtained assuming that the surface is composed mainly by Cu_2S. For this type of compounds (djurleite ($Cu_{1.94}S$) and low chalcocite (Cu_2S)) an average distance of 2.75 Å for neighboring copper ions is plausible.[17] For a compact hexagonal arrangement, this value implies that a maximum of $1.5 \cdot 10^{15}$ Cu atoms per cm^{-2} (geometric area) would be exposed to solution. On the other hand, we can estimate the real surface area of a monolayer of QDs by considering that a spherical particle has a surface area of $4\pi r^2$, occupying, in a compact hexagonal arrangement, an area of $2\sqrt{3}r^2$ (the contact area of the nanoparticles among them and with the substrate is neglected). Therefore, the real area is 3.6 times the geometric area ($2\pi/\sqrt{3}$). Consequently, the number of Cu atoms in the monolayer exposed to the electrolyte would be of $5.4 \cdot 10^{15}$ cm^{-2}, giving an overall charge of 865 $\mu C \cdot cm^{-2}$. By comparison with the experimental value, we realize that about 98 % of the Cu surface atoms would be oxidized (and dissolved).

References

1 H. Nakamura, W. Kato, M. Uehara, K. Nose, T. Omata, S. Otsuka-Yao-Matsuo, M. Miyazaki, H. Maeda, *Chem. Mater.* 2006, **18**, 3330.

2 K. Yoshino, K. Nomoto, A. Kinoshita, T. Ikari, Y. Akaki, Y. Yoshitake, *J. Mater. Sci: Mater. Electron* 2008, **19**, 301.

3 X. Tang, W. Cheng, E. Shi, G. Choo, J. Xue, *Chem. Commun*. 2011, **47**, 5217.

4 F. B. Courtel, R. W. Paynter, B. Marsan, M. Morin, *Chem. Mater*. 2009, **21**, 3752.

5 M. Uehara, K. Watanabe, Y. Tajiri,H. Nakamura, H. Maeda, *J. Chem. Phys.* 2008, **129**, 134709

6 G. Morell, R. S. Katiyar, S. Z. Weisz, T. Walter, H. W. Schock, I. Balberg, *Appl. Phys. Lett*. 1996**, 69**, 987.

7 K. Kampas, J. Spyridelis, M. Balkanski, *Phys. Stat. Sol. (b)* 1981, **105**, 291.

8 H. Tao, S. Mao, G. Dong, H. Xiao, X. Zhao, *Solid State Commun*. 2006, **137**, 408.

9 A. K. Shahi, B. K. Pandey, R. K. Swarnkar, R. Gopal, *Appl. Surf. Sci*. 2011, **257**, 9846.

10 F. Teng, Q. Liu, H. Zeng, *J. Colloid Interface Sci.* in press. DOI:10.1016/j.jcis.2011.10.048; I. Kartio, C. Basilio, R. H. Yoon, *Langmuir* 1998, **14**, 5274.

11 S. Shen, J. Chen, X. Wang, L. Zhao, L. Guo, *J. Power Sources* 2011, **196**, 10112.

12 W. Yue, S. Han, R. Peng, W. Shen, H. Geng, F. Wu, S. Tao, M. Wang, *J. Mater. Chem.* 2010, **20**, 7570.

13 P. Bera, S. Seok, *J. Solid State Chem.* 2010, **183**, 1872.

14 J. Llanos, A. Buljan, C. Mujica, R. Ramirez, *J. Alloys. Compd*. 1996, **234**, 40.

15 D. Shea, G. R. Helz, *Geochim. Cosmochim*. 1988, **52**, 1815.

16 C. A. Young, E. J. Dahlgren, R. G. Robins, *Hydrometallurgy* 2003, **68**, 23.

17 H. T. Jr. Evans, *Science* 1979, **203**, 356.